JACS
JOURNAL OF THE AMERICAN CHEMICAL SOCIETY
Article
pubs.acs.org/JACS

Asymmetric Free-Standing 2-D Photonic Crystal Films and Their Janus Particles

Jian-Tao Zhang, Xing Chao, and Sanford A. Asher*

Department of Chemistry, University of Pittsburgh, 219 Parkman Avenue, Pittsburgh, Pennsylvania 15260, United States

Supporting Information

ABSTRACT: We report the fabrication of large area, thin asymmetric free-standing two-dimensional (2-D) photonic crystals. We fabricate large area 2-D close-packed monodisperse polystyrene (PS) particle monolayers at air/water interfaces by using our needle tip flow method. We then layer tetraethyl orthosilicate (TEOS) onto the 2-D array to form a thin TEOS layer on the 2-D particle array on water. The hemispheres of PS particles located within the TEOS phase swell such that the adjacent particle hemispheres fuse. After TEOS evaporation, we obtain a free-standing connected photonic crystal film of hemispheres that efficiently diffracts light. The other side of the photonic crystal film consists of a fused connecting thin, flat sheet. Reactive ion etching (RIE) of the asymmetric films forms unusual, rough particle 2-D arrays and 2-D flower-like arrays. Mechanical abrasion allows one to separate the resulting novel Janus particles.

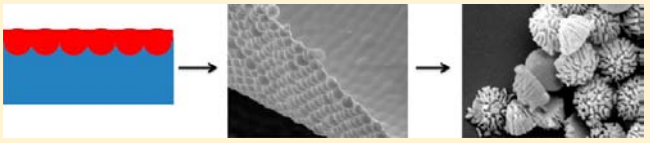

INTRODUCTION

Two-dimensional (2-D) nanostructured free-standing thin films are of interest because of their unique properties in areas such as optics, sensing devices, and separation membranes.[1−3] Free-standing films have been fabricated by layer-by-layer assembly,[1b,3] solution casting,[4] surfactant-assisted deposition,[5] and through filtration of dispersions of materials using membrane filters.[6] For example, Jiang et al. reported fabrication of composite membranes by spin-assisted layer-by-layer assembly on sacrificial substrates.[1b,3] Vendamme et al. reported the formation of a hybrid interpenetrating network (IPN) free-standing nanofilm by spin-coating a reaction solution of organic and inorganic precursors that were cross-linked to organic and inorganic networks.[7] Free-standing films have also been fabricated at liquid/air and liquid/liquid interfaces.[8−11]

The asymmetric chemical properties of Janus particles, for example, can be utilized for emulsion stabilization, while chemically anisotropic particles can be used for nanomotor propulsion.[12] Existing asymmetric structures include Janus spheres, micelles, rods, and discs. Asymmetric nanosheets are also useful because of their highly anisotropic shape and surface chemistry.[13] Chemically anisotropic nanosheets have been shown to achieve more stable emulsions than do Janus spheres, because the nanosheets better stabilize the emulsion by anchoring to the interfaces.[13a,b]

Yang et al. recently reported a technique for the large-scale fabrication of inorganic asymmetric nanosheets by crushing silica hollow spheres whose interior surface chemistry differs from that of its exterior.[13a] Fujii et al. described a method to make asymmetric films by forming 2-D particle arrays on top of aqueous solutions that contain reactive monomers that selectively polymerize at the water-exposed particle surface.[13b] It would be of great value to discover additional methods to form asymmetric materials for new applications.

In the work here, we demonstrate a facile approach to fabricate large asymmetric free-standing two-dimensional (2-D) crystalline colloidal array (CCA) films by fusing 2-D colloidal particle arrays at the air−water interface.

EXPERIMENTAL SECTION

600 nm diameter polystyrene (PS) particles were synthesized according to a previous method.[14] We utilized a PS suspension concentration of 20 wt % in water. The PS 2-D array on water was fabricated using the previously reported needle tip flow method.[15] Briefly, the PS dispersion and the 1-propanol were mixed at a ratio of 3:1 in volume. The PS suspension then was layered onto a water surface where the particles spread to assemble into a close-packed 2-D array at the air/water interface in a 9.5 cm diameter glass dish. Next 200 μL, 400 μL, or 800 μL of TEOS was carefully layered onto the 2-D PS array on the water surfaces. PS particles partially dissolved in the TEOS phase. 2-D asymmetric photonic colloidal crystal films formed upon TEOS evaporation in air. These films can be easily transferred to different substrates.

RIE treatment was carried out by using a Reactive Ion Etching System (RIE, Trion Technology Phantom III LT). Pure oxygen gas with a flow rate of 50 sccm was used as a plasma source to etch the photonic crystal array films at varying RIE durations. The ICP power and RF power are 300 and 30 W, respectively. The total pressure is 10 mTorr (1 Torr 133.3 Pa)

The asymmetric films on flat cover glass were sputter coated with a thin layer of Au, and the arrangement and surface morphology of the films was observed by using a scanning electron microscope (SEM, Joel JSM6390LV). The asymmetric film surface topography was measured by using an Asylum MFP-3D atomic force microscope (AFM, Bruker) in a tapping mode. TEM observations were carried out by using a transmission electron microscope (FEI Morgagni 268).

The contact angles were measured by using a VCA-OPTIMA drop shape analysis system (AST Products, Inc.). Liquid droplets (water

Received: June 5, 2013
Published: July 11, 2013

dx.doi.org/10.1021/ja405629k | J. Am. Chem. Soc. 2013, 135, 11397−11401

and TEOS) with a volume of 2 μL were used to measure the static contact angle. The measurement was performed in air at room temperature. Diffraction measurements were conducted at a fixed angle by utilizing an Ocean Optics USB4000 high-resolution spectrometer, a LS-1 tungsten halogen light source, and an R-series fiber optic reflection probe. The measurement was carried out in the Littrow configuration with a ~33° measurement angle between the probe and the normal to the 2-D array.

RESULTS AND DISCUSSION

Figure 1 illustrates our free-standing photonic crystal film fabrication method. We assemble a large 2-D array of colloidal

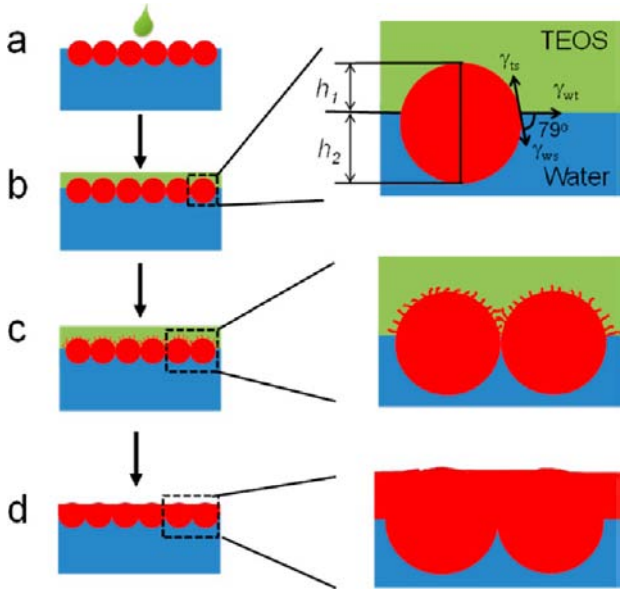

Figure 1. Preparation of asymmetric free-standing photonic crystal array film: (a) TEOS is layered onto the 600 nm diameter PS particle 2-D array prepared by the needle tip flow method; (b) a thin layer of TEOS forms on top of the PS particle array; (c) the PS particles in TEOS swell and partially dissolve; and (d) the neighboring particles fuse as the TEOS evaporates.

PS particles on a water surface by using our recently developed needle tip flow technique that spreads a dispersion of monodisperse PS particles in alcohol on a water surface. The particles self-assemble into a hexagonal close-packed 2-D array.[15] The close-packed 2-D array fills the water surface. We then layer ~200 μL of TEOS onto the 2-D array on the water surface (Figure 1a). The immiscible TEOS spreads to form a thin liquid layer that sandwiches the 2-D array between the TEOS layer and the water phase (Figure 1b). The PS particles swell and partially dissolve in the TEOS phase (Figure 1c), forming a continuous asymmetric free-standing 2-D photonic crystal film on the water after TEOS evaporation (Figure 1d). Here, we used a 9.5 cm diameter glass dish for the 2-D array fabrication, and added 200, 400, or 800 μL of TEOS to the 2-D array surfaces. We can fabricate larger films by using larger area water surfaces.

Figure 2a shows a photograph of a free-standing 2-D particle array film formed on a water surface. The film on the water surface is mechanically strong due to the fusing of neighboring particles, allowing it to be easily transferred from the water surface to substrates. Without fusing the particles, it is challenging to transfer the fragile free-standing 2-D particle array films.[15−17] Figure 2b and c shows a free-standing photonic

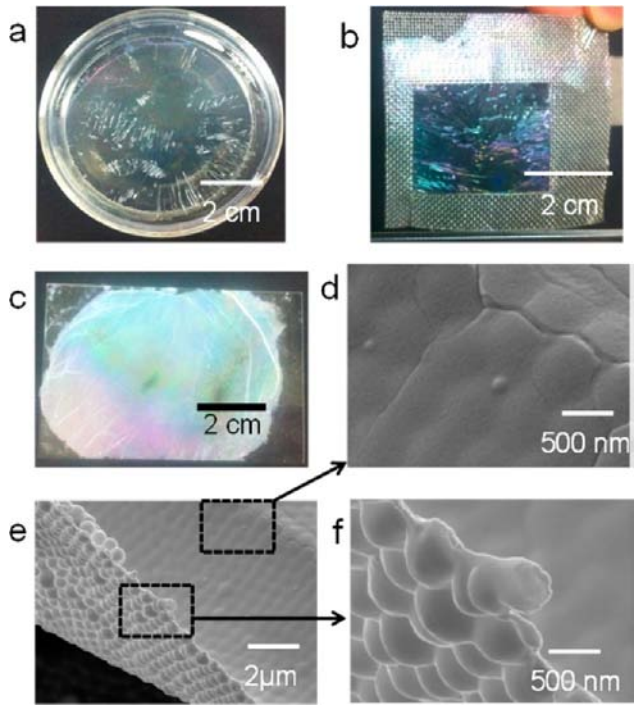

Figure 2. (a) Photograph of the 2-D CCA film formed on a water surface in 9.5 cm diameter glass dish formed by layering and evaporating 200 μL of TEOS. Photographs of asymmetric films transferred onto (b) metal mesh and (c) a flat glass slide; SEM images of the 2-D films showing asymmetric film (d) top surface, (e) edge view, and (f) bottom hemispherical array morphology.

crystal film that was transferred from the water surface to a metal mesh and to a glass substrate.

The free-standing photonic crystal film formation process must involve swelling and partial dissolution of the PS particles, and fusing of adjacent particle polymer regions. Our conclusion that the PS particles fuse derives from the flat thin film morphology of the resulting asymmetric films and from the observation that the diffraction from a 2-D PS array in contact with TEOS disappears within 1 h. Because the refractive index of TEOS is 1.38, refractive index matching cannot cause the diffraction to disappear. Only loss of the PS particle's refractive index modulation can cause the diffraction to disappear. The only simple mechanism leading to a modulation loss must be through fusing together of the PS particles to form a homogeneous PS slab.

TEOS is immiscible with water and has a smaller density (0.93 g/cm^3) than water (1.0 g/cm^3). TEOS spreads on the close-packed 2-D particle array on the water surface to form a thin liquid TEOS top layer (thickness ~30 μm for 200 μL of TEOS); the measured contact angle of TEOS with the 2-D PS array on a glass slide is too small to measure (<5°, data not shown). In contrast, the measured contact angle of water on the 2-D PS array is ~63°. Assuming negligible gravitational and buoyant forces at the TEOS/water interface, the particle positions at the interface equilibrate in recognition of the three interfacial tensions, following Young's equation:[18,19]

$$\gamma_{ws} = \gamma_{ts} - \gamma_{tw} \cos\theta \quad (1)$$

where θ is the contact angle at the three phase interface. γ_{ws}, γ_{ts}, and γ_{tw} are the interfacial tensions at the water/PS, TEOS/PS, and TEOS/water interfaces (Figure 1b, inset). The balance

dx.doi.org/10.1021/ja405629k | J. Am. Chem. Soc. 2013, 135, 11397−11401

between the interfacial tensions determines the PS particle location at the TEOS/water interface. We calculate the contact angle, θ, at the TEOS/water interface as 79° (see the Supporting Information). In this case, the particle thickness ratio in the TEOS phase relative to that of the water phase (h_1/h_2) is ~2:3 (Figure 1b).

The TEOS layer partially dissolves the PS particles (Figure 1c), causing them to swell and fuse.[20] After TEOS evaporation, we obtain free-standing thin 2-D array films on the water surface (Figure 1d). Although there might be a small amount of TEOS hydrolysis, we see no evidence of small SiO_2 particles.

Figure 2d–f shows SEM images of the highly asymmetric photonic crystal films. The top of the film that contacted the TEOS is relatively flat (Figure 2d), while the bottom of the film contacting water consists of a 2-D array of hemispherical protrusions (Figure 2f). Figure 3a and b shows 3-D tapping

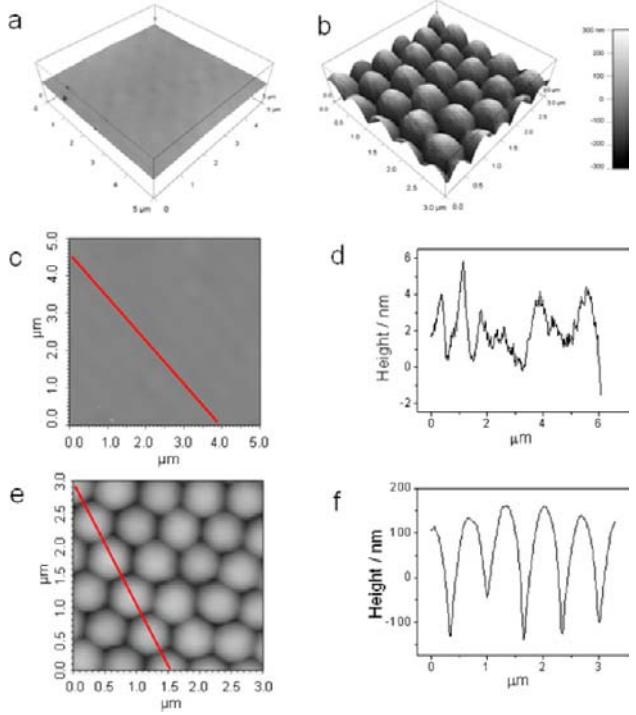

Figure 3. 3-D AFM height photographs of (a) top and (b) bottom surfaces of the asymmetric film; 2-D AFM topographs of the (c) top and (e) bottom of 2-D PS array and bottom of the 200 μL TEOS asymmetric film; (d) and (f) are AFM height profiles along indicated lines in (c) and (e) showing nearest neighbor particle spacings of 606 and 670 nm, and the roughness or <10 and >250 nm.

mode AFM images. The top homogeneous flat surface shows a roughness of <10 nm (Figure 3c and d). The bottom side containing the 2-D array of hemispheres shows a ~665 nm periodicity with a peak-to-trough height of >250 nm (Figure 3e and f).

Figure 4a–d shows the SEM images of the original PS array and the bottom of the free-standing films formed on water obtained by layering 200, 400, and 800 μL of TEOS on the top of 2-D particle arrays. For SEM of the film bottom side, we placed a dry glass slide onto the film surface upon which it adhered and removed the film from the water surface. For TEM, we placed a carbon-coated copper grid onto the film surface that adhered. We then lifted it from the water surface.

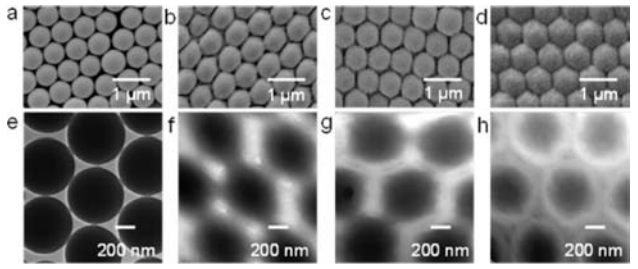

Figure 4. (a–d) SEM and (e,f) TEM images of (a,e) original PS array, and of free-standing films prepared by adding (b,f) 200 μL, (c,g) 400 μL, and (d,h) 800 μL of TEOS.

SEM and TEM (Figure 4e–h) of the original 2-D array show the expected hexagonal array of spherical particles. The PS particle surfaces appear crisp, and no bridging is evident between particles. In contrast, the TEOS contacted arrays show less TEM contrast, and the particles appear fuzzier as the amount of TEOS used increases. In addition, we see features indicating formation of neighboring particle interconnections that are associated with polymer filling the interstitial spaces.

The Figure 5a inset shows a photograph of the PS 2-D array and a free-standing asymmetric film on top of a front surface

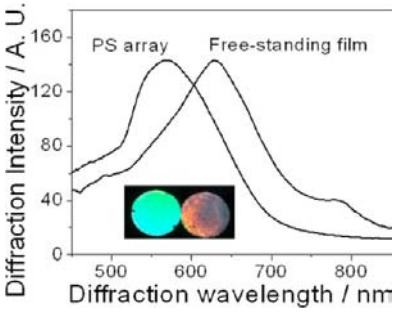

Figure 5. Diffraction of 2-D PS array and the asymmetric free-standing film on a reflective silver surface mirror. The diffraction measurements were carried out in a Littrow configuration, and the measurement angle between the probe and the normal to the 2-D array is ~33°. The inset shows an optical photograph taken at an angle of ~33° to the normal to the film.

silver mirror. The asymmetric films show strong light diffraction that is slightly weaker than that from the original PS array. The asymmetric film diffraction occurs at somewhat longer wavelengths because of a small increase in particle spacing induced by the TOES. The average particle spacing measured by AFM is 606 nm for the PS array and 667 nm for the film bottom hemispheres (Figure S1 in Supporting Information and Figure 3f).

The 2-D Bragg diffraction condition in the Littrow configuration is: $m\lambda = 3^{1/2}d \sin \phi$, where m is the diffraction order, λ is the wavelength of the diffracted light, d is the nearest neighboring particle spacing, and ϕ is the angle between the incident light and normal to the 2-D array.[21] Here, ϕ is ~33°. The 2-D diffraction wavelength of the original PS array and the asymmetric film should be λ = 571 and 629 nm, respectively, which agree well with the measured values (570 and 632 nm for PS and film, respectively).

Other solvents, such as cyclohexane, with similar properties can also be used for the free-standing film preparation. If we layer 200 μL of a good PS solvent, ethyl acetate, on the 2-D arrays on water, instead of TEOS, the PS particles completely

dx.doi.org/10.1021/ja405629k | J. Am. Chem. Soc. 2013, 135, 11397–11401

dissolve, and a completely homogeneous film forms on the water surface after the ethyl acetate evaporates (Supporting Information, Figure S2). The film does not diffract. Layering of 200 μL of TEOS followed by evaporation onto a 2-D SiO_2 particle array on water has no impact, indicating that the asymmetric free-standing film formation is caused by the fusing of the PS particles with a negligible contribution of any hydrolysis/condensation of TEOS.

We are able to utilize these asymmetric 2-D array films to fabricate a new class of Janus particles and a 2-D "flower-like" array by etching the asymmetric photonic crystal thin films described above. Reactive-ion etching (RIE) is a highly anisotropic etching technology for micro-/nanofabrication that uses reactive plasmas containing charged particles, excited neutrals, radicals, etc. RIE has been used to etch polymer surfaces and create size-controllable nonclose-packed PS arrays.[22] In the work here, we etched our photonic crystal array films by using oxygen RIE.

Figure 6a–d shows SEM images that monitor the impact of oxygen RIE etching of the original and the asymmetric 2-D

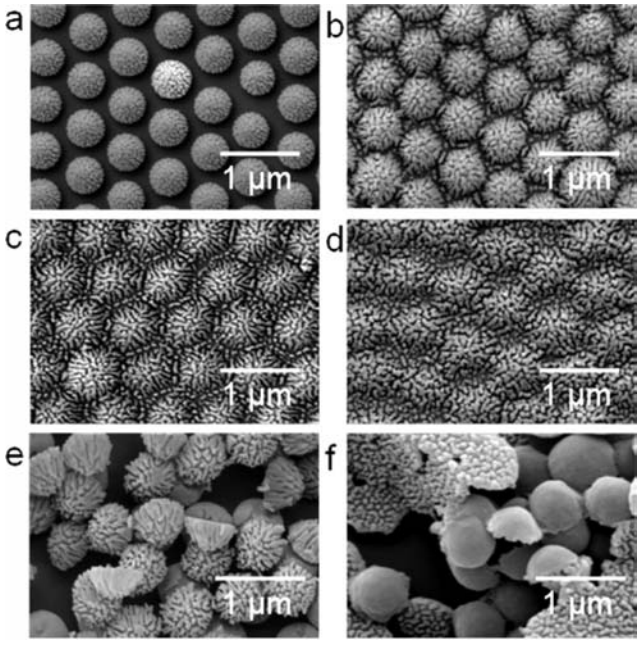

Figure 6. SEM micrographs measured after 3 min of reactive ion etching (RIE) treatment of (a) PS array, and asymmetric films prepared by adding (b) 200 μL, (c) 400 μL, and (d) 800 μL of TEOS to the top surface. SEM images of 200 μL TEOS films after 3 min with RIE treatment of asymmetric film (e) bottom side and (f) top side. Individual Janus particles are released from asymmetric film. In (e) the hemispheres are roughened and the back of the hemispherical particles was protected. In (f) the hemispheres are protected and the back of the film particle surface is rough.

arrays. Three minutes RIE of the original 2-D array films results in an obvious roughening of the particles and decreased particle diameters. The particles are no longer close-packed, and the particles are likely now not spherical.[22] The surfaces of the PS array and the films treated for 3 min are rough, similar to the morphology reported for poly(ethylene terephthalate).[23]

Figure 6b–d shows the increasing roughening and the formation of bumps on the asymmetric film particle surfaces after 3 min RIE. The degree of RIE roughening of the PS arrays seems to increase with the amount of TEOS used to prepare the asymmetric free-standing films. However, any clear conclusions are confounded by the fact that the hemispherical protrusion heights decrease with the amount of TEOS used. Figure 6e and f shows that RIE of our asymmetric 2-D particle array films results in fragmentation into their individual constituent particles. Figure 6e shows Janus particles formed by RIE of the protruding hemispherical arrays where the rough surface is the eroded hemispherical surface. In contrast, Figure 6f shows Janus particles formed by irradiation of the back of the asymmetric films, where the thin back of the protrusions is eroded. Increasing the RIE time over 4 min fractures the system to form individual particles.

The RIE etching mechanism can be considered as a process where polymer degradation results in a low molecular weight liquid film that dewets the polymer causing complex morphologies.[22] RIE chain scission produces a liquid layer of low-molecular-weight fragments on the immobile PS solid surface. Rayleigh instabilities arise to form protrusions on the surface because the low-molecular-weight fragments dewet the PS surface.[22]

Increasing the RIE treatment time causes increased erosion of the asymmetric film and the PS protrusions. Figure 7 shows

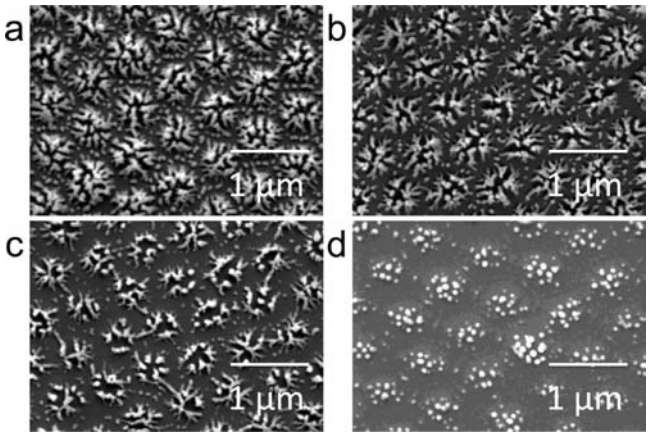

Figure 7. SEM images of 200 μL TEOS free-standing asymmetric photonic crystal films after (a) 6, (b) 10, (c) 20, and (d) 40 min RIE treatment.

SEM images of an asymmetric film formed with the use of 200 μL of TEOS treated for 6, 10, 20, and 40 min, respective. We find that the flower pattern area decreases and the flowers show deeper grooves as the etching time increases. The 2-D patterns etched for 6, 10, and 20 min surprisingly show hollow grooves that are caused by the Rayleigh instability.[23]

RIE treatment does not destroy the 2-D ordered structures; therefore, the RIE treated films still show 2-D diffraction. Three minutes RIE treated PS particle arrays and Janus films show strong diffraction (Supporting Information, Figure S3a), quite similar to the untreated PS array and free-standing films. As shown in Figure S3b, the diffraction intensity of the films prepared by adding 200 μL of TEOS decreases with increasing RIE time. It is difficult to observe the diffraction from the films treated with 20 and 40 min RIE because of the decrease in the refractive index modulation of the monolayer films that is caused by the thinning 2-D PS structures.

In conclusion, we prepared large area asymmetric free-standing 2-D thin photonic crystal films by adding TEOS to a close-packed 2-D PS particle array located at the TEOS/water interface to partially dissolve and fuse the particle array. TEOS

evaporation leaves behind a rugged thin, free-standing film at the air/water interface that is smooth on the TEOS exposure side and consists of a 2-D array of hemispherical PS protrusions on the water side. RIE roughens the particle surfaces, resulting in Janus particles.

■ ASSOCIATED CONTENT

Supporting Information

AFM topography image of the asymmetric film top surface; SEM image of the bottom side film obtained by layering 200 μL of ethyl acetate on PS 2-D array on water; optical photographs showing the 2-D diffraction of the RIE treated films; and calculation of contact angles at the three-phase interface. This material is available free of charge via the Internet at http://pubs.acs.org

■ AUTHOR INFORMATION

Corresponding Author

asher@pitt.edu

Notes

The authors declare no competing financial interest.

■ ACKNOWLEDGMENTS

We gratefully acknowledge HDTRA for funding support (Grant no. 1-10-1-0044).

■ REFERENCES

(1) (a) Cheng, W.; Campolongo, M. J.; Tan, S. J.; Luo, D. *Nano Today* **2009**, *4*, 482−493. (b) Jiang, C.; Tsukruk, V. V. *Adv. Mater.* **2006**, *18*, 829−840.

(2) Mueggenburg, K. E.; Lin, X. M.; Goldsmith, R. H.; Jaeger, H. M. *Nat. Mater.* **2007**, *6*, 656−60.

(3) Jiang, C.; Markutsya, S.; Pikus, Y.; Tsukruk, V. V. *Nat. Mater.* **2004**, *3*, 721−728.

(4) Feng, D.; Lv, Y.; Wu, Z.; Dou, Y.; Han, L.; Sun, Z.; Xia, Y.; Zheng, G.; Zhao, D. *J. Am. Chem. Soc.* **2011**, *133*, 15148−15156.

(5) Jin, J.; Wakayama, Y.; Peng, X.; Ichinose, I. *Nat. Mater.* **2007**, *6*, 686−691.

(6) Peng, X.; Jin, J.; Ericsson, E. M.; Ichinose, I. *J. Am. Chem. Soc.* **2007**, *129*, 8625−8633.

(7) Vendamme, R.; Onoue, S. Y.; Nakao, A.; Kunitake, T. *Nat. Mater.* **2006**, *5*, 494−501.

(8) Lin, Y.; Skaff, H.; Böker, A.; Dinsmore, A. D.; Emrick, T.; Russell, T. P. *J. Am. Chem. Soc.* **2003**, *125*, 12690−12691.

(9) Duan, H. W.; Wang, D.; Kurth, D.; Möhwald, H. *Angew. Chem., Int. Ed.* **2004**, *43*, 5639−5642.

(10) Xia, H.; Wang, D. *Adv. Mater.* **2008**, *20*, 4253−4256.

(11) Yan, F.; Goedel, W. A. *Adv. Mater.* **2004**, *16*, 911−915.

(12) (a) Walther, A.; Mueller, A. H. E. *Soft Matter* **2008**, *4*, 663−668. (b) Jiang, S.; Chen, Q.; Tripathy, M.; Luijten, E.; Schweizer, K. S.; Granick, S. *Adv. Mater.* **2010**, *22*, 1060−1071.

(13) (a) Liang, F. X.; Shen, K.; Qu, X. Z.; Zhang, C. L.; Wang, Q.; Li, J. L.; Liu, J. G.; Yang, Z. Z. *Angew. Chem., Int. Ed.* **2011**, *50*, 2379−2382. (b) Yang, H.; Liang, F.; Wang, X.; Chen, Y.; Zhang, C.; Wang, Q.; Qu, X.; Li, J.; Wu, D.; Yang, Z. *Macromolecules* **2013**, DOI: 10.1021/ma400261y. (c) Fujii, S.; Kappl, M.; Butt, H. J.; Sugimoto, T.; Nakamura, Y. *Angew. Chem., Int. Ed.* **2012**, *51*, 9809−9813.

(14) Reese, C.; Asher, S. A. *J. Colloid Interface Sci.* **2002**, *248*, 41.

(15) Zhang, J. T.; Wang, L.; Lamont, D. N.; Velankar, S.; Asher, S. A. *Angew. Chem., Int. Ed.* **2012**, *51*, 6117−6120.

(16) (a) Zhang, J.; Li, Y.; Zhang, X.; Yang, B. *Adv. Mater.* **2010**, *22*, 4249−4269. (b) Yang, S.; Lei, Y. *Nanoscale* **2011**, *3*, 2768. (c) Ye, X.; Qi, L. *Nano Today* **2011**, *6*, 608−631.

(17) Cheng, W. L.; Campolongo, M. J.; Cha, J. J.; Tan, S. J.; Umbach, C. C.; Muller, D. A.; Luo, D. *Nat. Mater.* **2009**, *8*, 519−525.

(18) (a) Reed, K. M.; Borovicka, J.; Horozov, T. S.; Paunov, V. N. *Langmuir* **2012**, *28*, 7291−7298. (b) Tadmor, R. *Langmuir* **2004**, *20*, 7659−7664.

(19) Adamson, A. W.; Gast, A. P. *Physical Chemistry of Surfaces*, 6th ed.; Wiley: New York, 1997.

(20) Yu, J.; Geng, C.; Zheng, L.; Ma, Z.; Tan, T.; Wang, X.; Yan, Q.; Shen, D. *Langmuir* **2012**, *28*, 12681−12689.

(21) (a) Zhang, J. T.; Wang, L.; Luo, J.; Tikhonov, A.; Kornienko, N.; Asher, S. A. *J. Am. Chem. Soc.* **2011**, *133*, 9152−9155. (b) Tikhonov, A.; Kornienko, N.; Zhang, J. T.; Wang, L.; Asher, S. A. *J. Nanophotonics* **2012**, *6*, 063509−1−9.

(22) (a) Choi, D. G.; Yu, H. K.; Jang, S. G.; Yang, S. M. *J. Am. Chem. Soc.* **2004**, *126*, 7019−7025. (b) Vogel, N.; Goerres, S.; Landfester, K.; Weiss, C. K. *Macromol. Chem. Phys.* **2011**, *212*, 1719−1734. (c) Tan, J. Y.; Sow, C. H.; Lim, K. Y.; Cheong, F. C.; Chong, G. L.; Wee, A. T.S.; Ong, C. K. *J. Phys. Chem. B* **2004**, *108*, 18575−18579. (d) Fujimura, T.; Tamura, T.; Itoh, T.; Haginoya, C.; Komori, Y.; Koda, T. *Appl. Phys. Lett.* **2001**, *78*, 1478−1450. (e) Yang, J. W.; Sim, J. I.; An, H. M.; Kim, T. G. *J. Korean Phys. Soc.* **2011**, *58*, 994−997.

(23) Powell, H. M.; Lannutti, J. J. *Langmuir* **2003**, *19*, 9071−9078.